

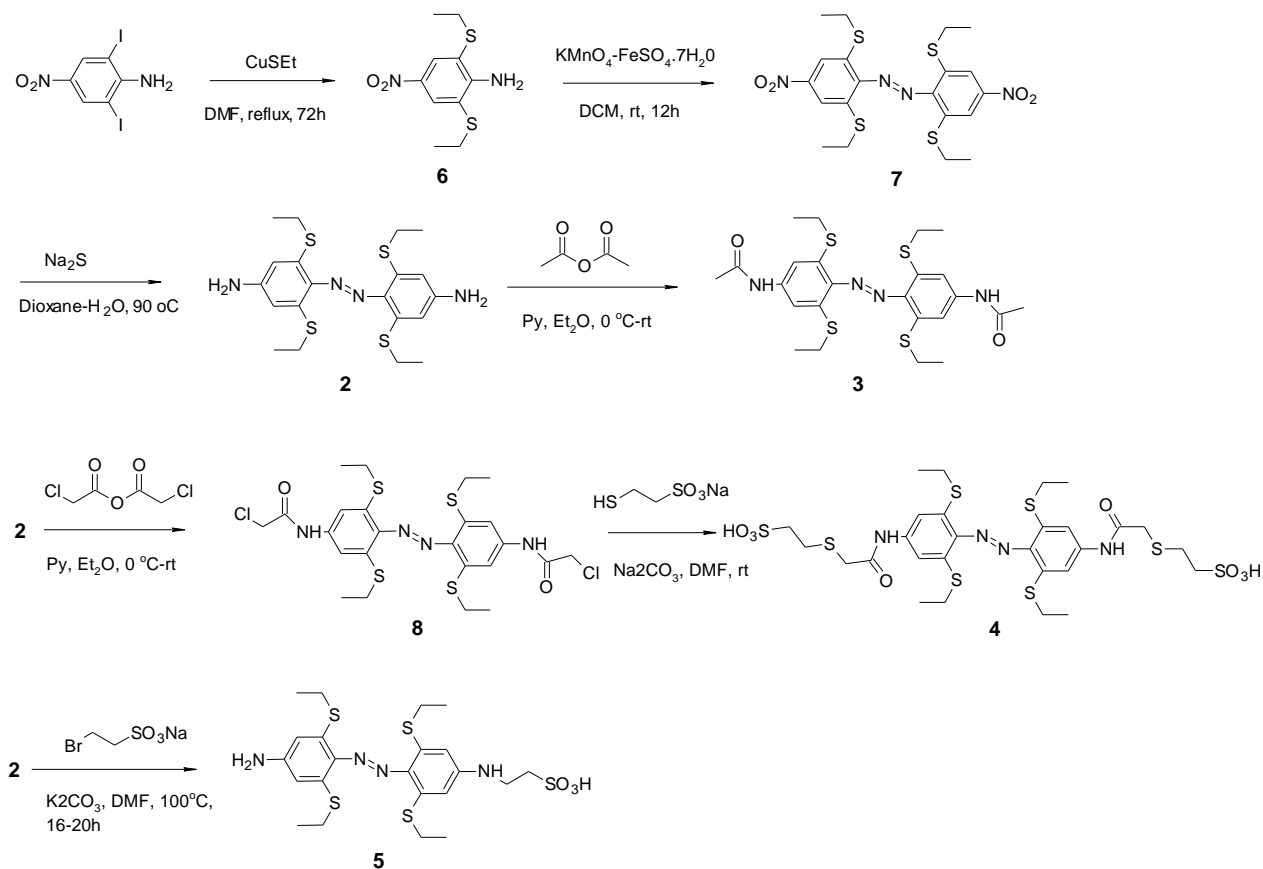
Robust visible light photoswitching with *ortho*-thiol substituted azobenzenes

Subhas Samanta, Theresa M. McCormick, Simone K. Schmidt, Dwight S. Seferos, G. Andrew Woolley,*

Department of Chemistry, University of Toronto, 80 St. George St. Toronto, ON M5S 3H6, Canada.

Supporting Information

Synthesis: The *o*-tetra-SEt substituted azobenzene derivatives **2**, **3**, **4** and **5** were synthesized as outlined in the scheme below:



Synthesis of 2,6-dithioethyl-4-nitroaniline (6): A mixture of 2,6-diiodo-4-nitroaniline (8.0 g, 20.5 mmol) and CuSEt (10.0 g, 80.2 mmol) in DMF (180 mL) was heated at 135°C for 60h. After cooling the solution was diluted with Et_2O (10 mL), filtered through celite and washed with

Et₂O. The combined organic layers were washed with H₂O and saturated NaCl solution, dried over anhyd. Na₂SO₄, filtered and concentrated. Purification by flash silica gel column chromatography under a nitrogen atmosphere led to **6** (2.2 g, 45% yield) as a yellow crystalline solid. ¹H NMR (400 MHz, CDCl₃): δ ppm 1.24 (t, *J* = 7.6 Hz, 6H), 2.82 (q, *J* = 7.6 Hz, 4H), 5.78 (br, NH), 8.22 (s, 2H); ¹³C NMR (100 MHz, CDCl₃): δ ppm 15.0, 29.4, 117.7, 131.1, 137.9, 154.9; ESI-HRMS: *m/z* calcd for C₁₀H₁₄N₂O₂S₂: 258.04912 [M]⁺; found: 258.04833.

Synthesis of 2,2',6,6'-tetraethylthio-4,4'-dinitroazobenzene (7): To a suspension of 2,6-dithioethyl-4-nitroaniline **6** (1.1 g, 4.3 mmol) in dichloromethane (80 mL) was added 4.6 g of a pre-ground (1:1) mixture of FeSO₄ × 7 H₂O and KMnO₄ under nitrogen gas atmosphere. The reaction was vigorously stirred under reflux for 12 h. After cooling to room temperature, the brown suspension was filtered through celite and washed with CH₂Cl₂. The crude product was subjected to flash silica gel column chromatography to obtain **7** (0.045 g, 2.1% yield) as a dark purple solid. ¹H NMR (400 MHz, CDCl₃): δ ppm 1.37 (t, *J* = 7.6 Hz, 12H), 3.02 (q, *J* = 7.6 Hz, 8H), 7.93 (s, 4H); ¹³C NMR (100 MHz, CDCl₃): δ ppm 13.2, 27.3, 116.3, 140.0, 147.8, 148.5; ESI-HRMS: *m/z* calcd for C₂₀H₂₅N₄O₄S₄: 513.07586 [M+H]⁺; found: 513.07084.

Synthesis of 2,2',6,6'-tetraethylthio-4,4'-diaminoazobenzene (2): To a solution of **7** (76.0 mg, 0.15 mmol) in a mixture of dioxane/EtOH/H₂O (15 mL:4 mL:1 mL) was added Na₂S (250 mg, 3.0 mmol) and the solution was heated to 85-90°C for 12 h. The completion of the reaction was judged by TLC analysis. After cooling, the solvent was removed by rotary evaporation; the residue was dissolved in EtOAc and extracted with H₂O and brine. The combined organic layer was dried over anhyd. Na₂SO₄, filtered and concentrated in vacuo. Purification by silica gel column chromatography gave **2** (35.0 mg; 52 %) as a dark red solid. ¹H NMR (400 MHz, DMSO-*d*₆): δ ppm 1.22 (t, *J* = 7.2 Hz, 12H), 2.77 (q, *J* = 7.2 Hz, 8H), 5.73 (br, NH), 6.35 (s, 4H); ¹³C NMR (125 MHz, DMSO-*d*₆): δ ppm 13.3, 25.2, 105.9, 137.0, 137.2, 149.1; ESI-HRMS: *m/z* calc'd for C₂₀H₂₉N₄S₄: 453.1269 [M+H]⁺; found: 453.1255.

Synthesis of 2,2',6,6'-tetraethylthio-4,4'-diacetamidoazobenzene (3): To an ice-cold solution of **2** (16 mg, 0.035 mmol) in pyridine (2 mL) was added acetic anhydride (144 mg, 134 μL, 0.14

mmol) and the mixture was stirred at room temperature for 12h. Then the solvent was removed by rotary evaporation and the residue obtained was precipitated from a DMF/H₂O solvent mixture to yield **3** (17.0 mg, 89% yield) as a red solid. ¹H NMR (400 MHz, DMSO-*d*₆): δ ppm 1.25 (t, *J* = 7.2 Hz, 12H), 2.10 (s, 6H), 2.85 (q, *J* = 7.2 Hz, 8H), 7.53 (s, 4H), 10.21 (s, NH); ¹³C NMR (125 MHz, DMSO-*d*₆): δ ppm 13.3, 24.3, 25.6, 111.2, 136.9, 140.3, 141.2, 169.0; ESI-HRMS: *m/z* calcd for C₂₄H₃₃N₄O₂S₄: 537.1480 [M+H]⁺; found: 537.1463.

Synthesis of 2,2',6,6'-tetraethylthio-4,4'-bis(chloroacetamido)azobenzene (8):

To an ice-cold solution of **2** (1.5 mg, 3.3 μmol) in an ether/pyridine (0.5:0.3 mL) mixture was added dropwise a solution of chloroacetic anhydride (2.0 mg, 9.9 μmol) in ether (0.3 mL). The resulting solution was warmed to room temperature and allowed to stir for 1h. The orange precipitate obtained was filtered and washed with ether thoroughly. The product **8** (1.7 mg, 85% yield) was pure enough to use for the next step. ¹H NMR (400 MHz, DMSO-*d*₆): δ ppm 1.27 (t, *J* = 7.2 Hz, 12H), 2.87 (q, *J* = 7.2 Hz, 8H), 4.33 (s, 4H), 7.54 (s, 4H), 10.57 (s, NH); ¹³C NMR (125 MHz, DMSO-*d*₆): δ ppm 13.3, 25.6, 43.7, 111.6, 137.2, 139.6, 141.6, 165.3; ESI-HRMS: *m/z* calc'd for C₂₄H₃₁Cl₂N₄O₂S₄: 605.0701 [M+H]⁺, found: 605.0696.

Synthesis of 2,2',6,6'-tetraethylthio-4,4'-bis(2-sulfoethylthio)acetamido)azobenzene (4):

A mixture of **8** (1.0 mg, 1.65 μmol), sodium 2-mercaptoethanesulfonate (0.6 mg, 3.66 μmol) and sodium carbonate (3 mg, 0.03 mmol) in 300 μL DMF was stirred at room temperature for 12h. The formation of the desired product **4** was confirmed by ESI-mass analysis of the reaction mixture. It was then purified by reversed phase by reverse-phase HPLC on a semi-preparative RX-C8 column (Zorbax, 9.4 mm ID x 255 mm) using a linear gradient of 10-70% acetonitrile/H₂O (containing 0.1% trifluoroacetic acid) over the course of 30 min; elution at 48% acetonitrile. ¹H NMR (600 MHz, 0.62 mM phosphate buffer, pH 7 in D₂O at 20°C): δ ppm 1.17 (t, *J* = 7.2 Hz, 12H), 2.79 (t, *J* = 7.2 Hz, 4H), 2.83 (q, *J* = 7.2 Hz, 8H), 3.01 (t, *J* = 7.2 Hz, 4H), 3.25 (s, 4H), 7.22 (s, 4H); ESI-HRMS: *m/z* calc'd for C₂₈H₃₉N₄O₈S₈: 815.0539 [M-H]⁻, found: 815.0518.

Synthesis of 2,2',6,6'-tetraethylthio-4-amino-4'-(2-sulfoethylamino)azobenzene (5)

A mixture of **2** (20.0 mg, 0.04 mmol), sodium 2-bromoethanesulfonate (15.0 mg, 0.07 mmol) and potassium carbonate (12.0 mg, 0.09 mmol) in 2.5 mL DMF was stirred at 100°C over a period of 24h. The formation of the desired product **5** was confirmed by ESI-mass analysis of the reaction mixture. It was then purified by reversed phase by reverse-phase HPLC (RX-C8 column as described above) using a linear gradient of 10-75% acetonitrile/H₂O (containing 0.1% trifluoroacetic acid) over the course of 25 min; elution at 57.5% acetonitrile. ¹H NMR (400 MHz, DMSO-*d*₆): δ ppm 1.21-1.25 (m, 12H), 2.69 (t, *J* = 7.2 Hz, 2H), 2.74-2.83 (m, 8H), 3.37 (t, *J* = 7.2 Hz, 2H), 6.29 (s, 2H), 6.43 (s, 2H); ¹³C NMR (125 MHz, DMSO-*d*₆): δ ppm 25.0, 46.5, 114.2, 119.1, 119.7, 124.3, 125.1, 135.8, 136.7, 144.2, 146.6, 152.4, 167.8; ESI-HRMS: *m/z* calc'd for C₂₂H₃₁N₄O₃S₅: 559.1005 [M-H]⁻, found: 559.1015.

Spectra and Photoisomerization:

1) UV/Vis absorption spectra, thermal cis-to-trans relaxation rates and photobleaching study of (2): UV-Vis absorbance spectra and thermal relaxation data for cis isomers in various solvents were obtained on a diode array UV-Vis spectrophotometer (Ocean Optics Inc., USB4000) coupled to a temperature controlled cuvette holder (Quantum Northwest, Inc.) (Fig. S1). Spectra were acquired in a 1 cm path length quartz cuvette. At an angle of 90° to the measuring beam, the samples were irradiated with LEDs emitting at 407 nm or 423 nm or 450 nm or 518 nm until no further decrease in absorbance was observed. Since significant photoswitching was observed in acetonitrile (ACN) and dimethylsulfoxide (DMSO), the thermal cis-to-trans isomerisation rates were measured in these solvents. Increase in absorption after removing the blue light source (423 nm or 450 nm) was measured as a function of time and the resulting curves were fitted with mono-exponential functions. Half lives of the cis isomers are given in Fig. S2. To check the stability to photobleaching, a solution of (**2**) in DMSO was exposed alternately to blue light (423 nm) and heat (25°C). After a period of 2 hours, insignificant photobleaching was observed (Fig. S3).

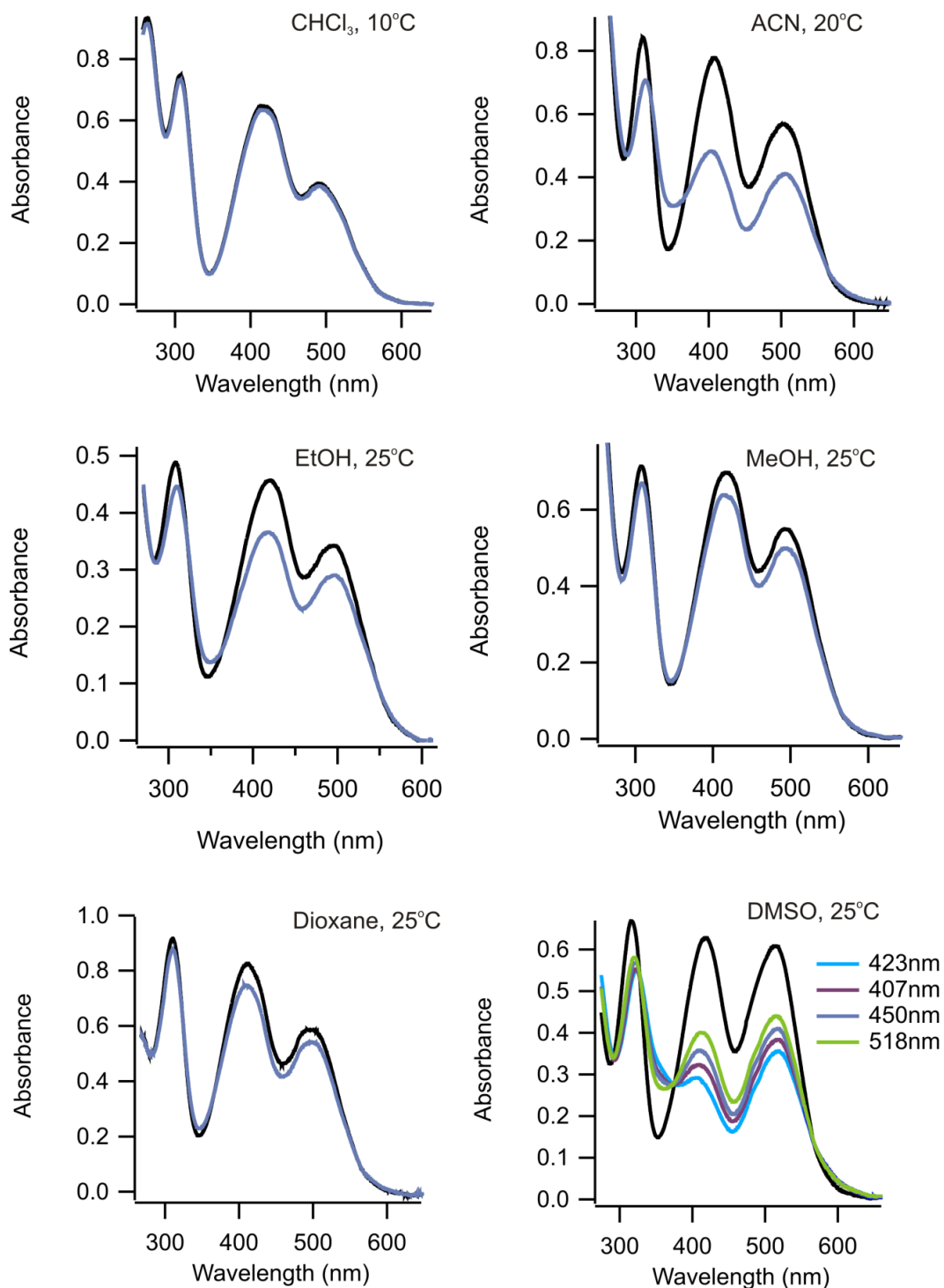


Fig. S1. UV-Vis absorption spectra of (2) in various solvents (indicated): dark-adapted spectra (black lines) and steady state spectra under blue (450 nm) light illumination (blue lines). Steady state spectra in DMSO were obtained under violet (407 nm), blue (423 nm and 450 nm) and green (518 nm) light irradiations.

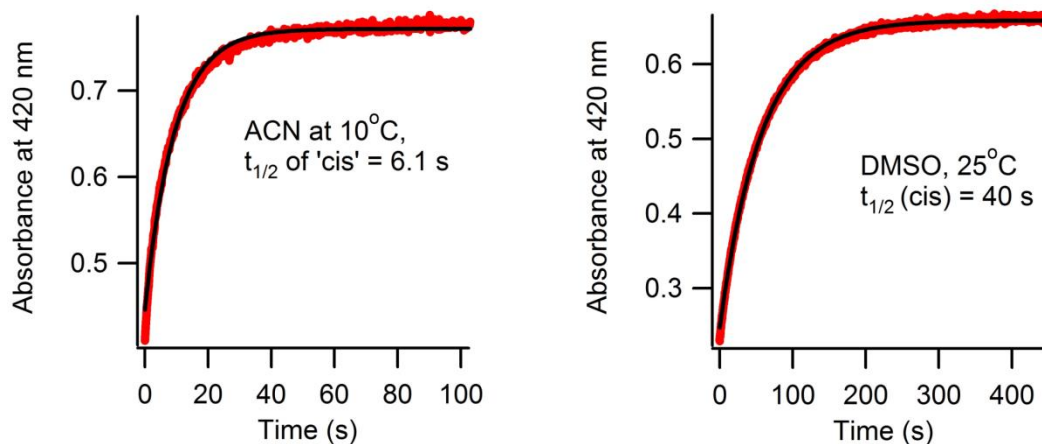


Fig. S2. Thermal cis-to-trans relaxation rates of **(2)** in ACN and DMSO at 10°C and 20°C, respectively. Black lines represent mono-exponential fits of the experimental data (red lines).

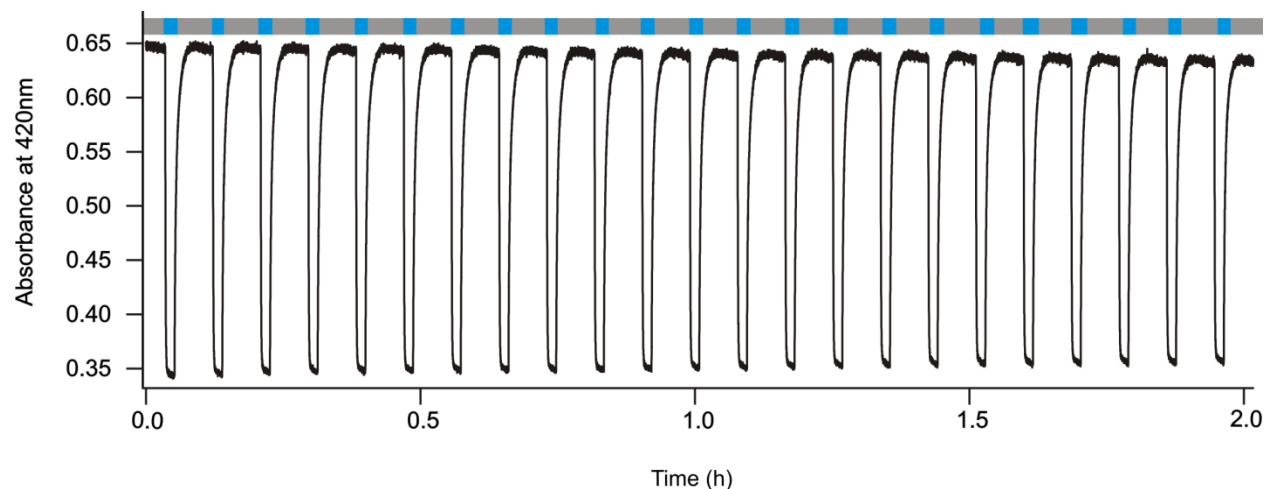


Fig. S3. Multiple rounds of photoswitching of **(2)** in DMSO solution upon exposure to blue light (423 nm)(blue boxes) followed by thermal relaxation at 25°C (gray colored boxes).

2) Molar extinction coefficient determination for compounds (2) and (3): To obtain the molar extinction coefficients, ^1H NMR spectra of **(2)** and **(3)** in $\text{DMSO-}d_6$ were recorded with a known concentration of 1,2-dichloroethane as internal standard. Samples with known concentrations were then used to record the UV/Vis absorption spectra to calculate the molar extinction coefficients. The absorption coefficients in DMSO were calculated to be $10,900 \text{ M}^{-1} \text{ cm}^{-1}$ (415 nm) and $10,600 \text{ M}^{-1} \text{ cm}^{-1}$ (512 nm) for **(2)**, and $16,600 \text{ M}^{-1} \text{ cm}^{-1}$ (417 nm) and $7,100 \text{ M}^{-1} \text{ cm}^{-1}$ for **(3)**.

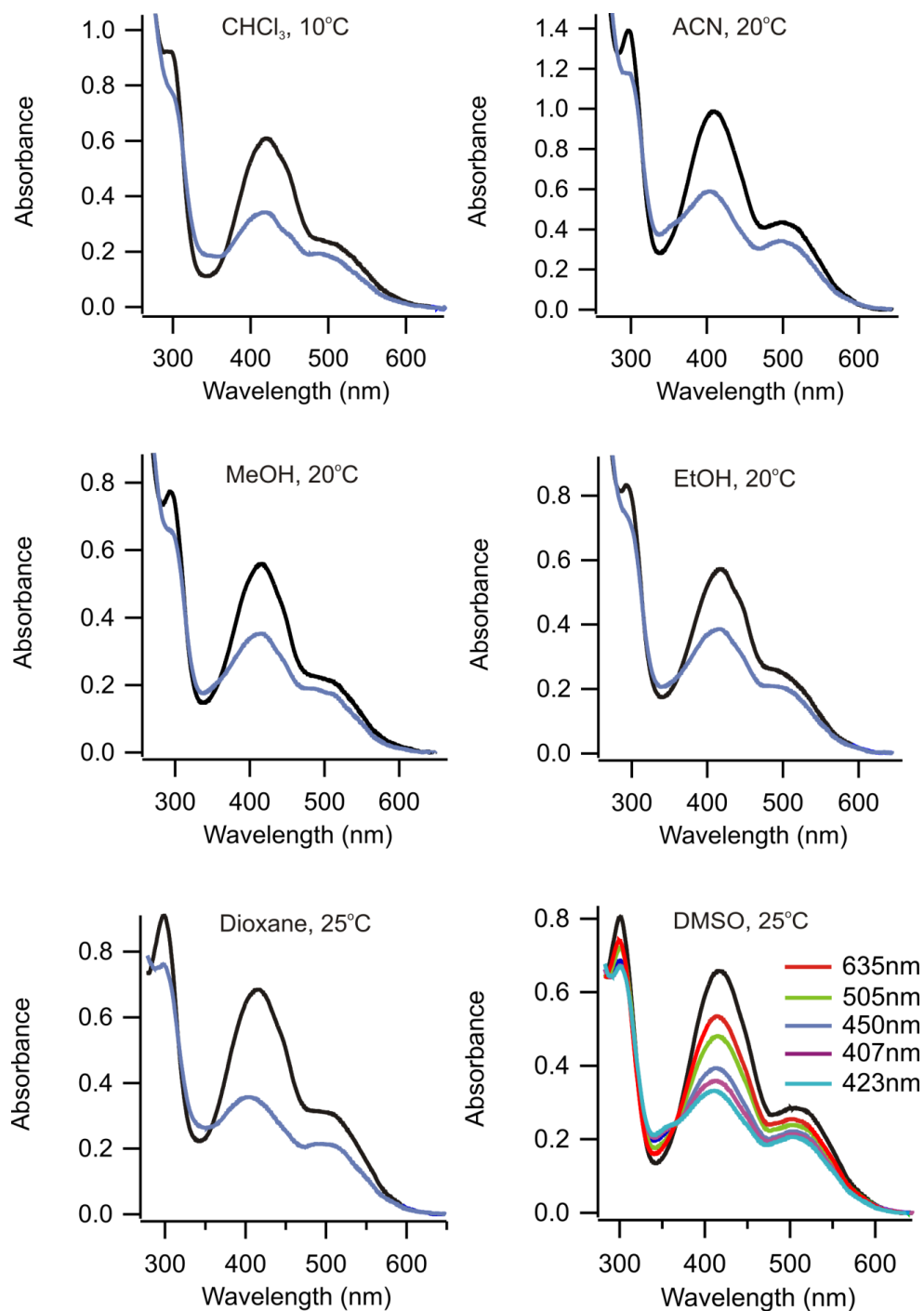


Fig. S4. UV-Vis absorption spectra of (**3**) in various solvents (indicated): dark-adapted spectra (black lines) and steady state spectra under blue (450 nm) light illumination (blue lines). Steady state spectra in DMSO were obtained under violet (407 nm), blue (423 nm and 450 nm), green (505 nm) and red (635 nm) light irradiation.

3) UV/Vis absorption spectra and thermal cis-to-trans relaxation rates of (3): UV/Vis absorbance spectra (for dark-adapted and irradiated states acquired with various visible light exposures) and relaxation rates for the cis isomers in various solvents were acquired in a similar manner as for (2) on a diode array UV–Vis spectrophotometer (Ocean Optics Inc., USB4000) (Fig. S4 and S5).

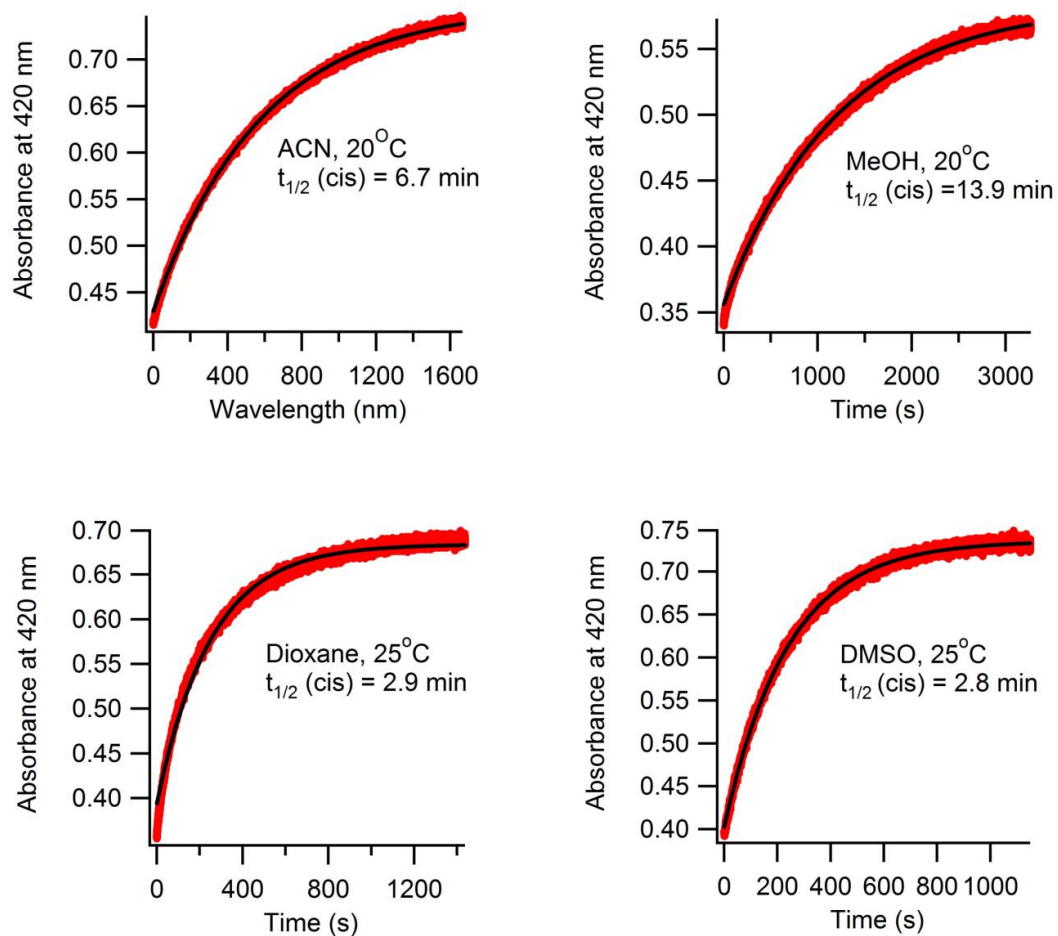


Fig. S5. Thermal cis-to-trans relaxation rates for (3) under various conditions (indicated): black lines represent mono-exponential fits of the experimental data (red lines).

4) UV/Vis absorption spectra and thermal cis-to-trans relaxation rates for (4):

UV/Vis absorbance spectra for the dark-adapted and irradiated states of (4) in 1 mM phosphate buffer pH 7 were acquired by using Perkin-Elmer Lambda 35 spectrophotometer. Isomerization was observed with blue light (423 nm) leading to 70% cis isomer and red light (635 nm) producing 59% cis (Fig. 6A)(see section 5 (SI) for how these percentages were calculated). Photostationary states at various temperatures upon blue light irradiation, acquired on a diode array UV-Vis spectrophotometer (Ocean Optics Inc., USB4000), showed that higher temperature enhanced switching efficiency to some extent (Fig. 6B). Rates of thermal cis-to-trans isomerization at different temperatures were obtained with a Perkin-Elmer Lambda 35 instrument by acquiring scans as a function of time after irradiation with either blue or red light (Fig. S7).

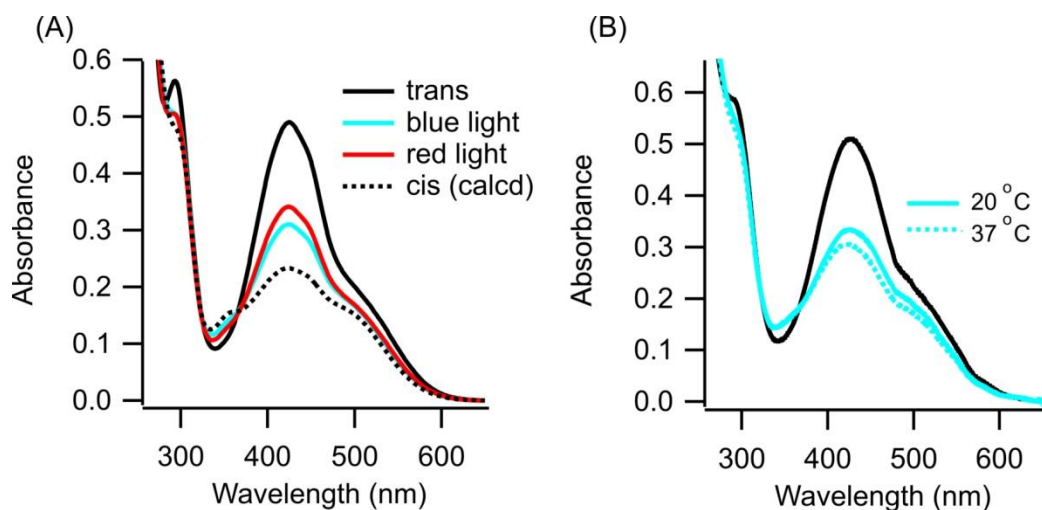


Fig. S6. (A) UV/Vis absorption spectra of (4) in 1 mM phosphate buffer (pH 7): dark-adapted (black line), upon exposure to 423 nm light (blue line) and 635 nm light (red lines), calculated cis spectra (dotted line)(see section 5 of SI). (B) UV/Vis absorption spectra of (4) upon exposure to 423 nm light at 20°C (solid blue line) and 37°C (dotted blue line).

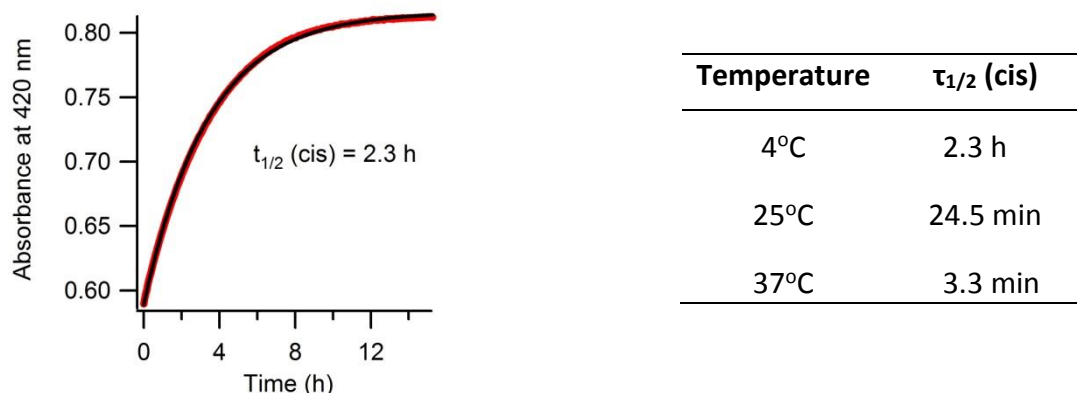


Fig. S7. Thermal cis-to-trans relaxation rate of **(4)** in 1 mM phosphate buffer (pH 7) at 4°C (left panel). The half lives of the cis isomer at various temperatures are tabulated in the right panel.

5) Calculation of cis spectra and cis percentages at the photostationary states for **(3)** and **(4)**:

Since the cis isomer of **(4)** exhibited more thermal stability than that of **(3)**, the former was used to calculate the cis isomer spectrum as well as the cis percentage in the steady state using 1D proton NMR and UV/Vis absorption spectra. A NMR tube containing a 0.1 mM solution of **(4)** in phosphate buffer (0.6 mM, pH 7, in D₂O) was irradiated with 423 nm light for 10 minutes while rotating the tube. Then, under dark conditions, the sample was quickly placed into the NMR spectrometer (600 MHz), maintained at 20°C, and the proton spectrum was recorded. The experiment was repeated three times maintaining a 5 min time gap between turning off irradiation and FID acquisition. The cis isomer content measured under these conditions was calculated to be 46% by comparing the signal intensities of methyl protons of ortho-thioethyl groups (highlighted) for both isomers (Fig. S8). In a similar manner, the sample was irradiated in the NMR tube for 10 minutes and then, after allowing the sample to relax in the dark for 5 min at 20°C, the UV/Vis absorption spectra was recorded on a Perkin-Elmer Lambda 35 spectrophotometer using a 0.15 cm path length cuvette. The resulting absorption spectrum is expected to be composed of 46% cis and 54% trans isomers (Fig. S8B). This spectrum in combination with the trans one (dark-adapted) permits calculation of the cis spectrum of **(4)** and **(3)**(Fig. 1c). The percentage of cis isomers with steady state irradiation of **(3)** in DMSO and

(4) in a relatively dilute solution (34 μM) in 1 mM phosphate buffer pH 7 were calculated to be ~70% (Fig. S6, Fig. 1c)

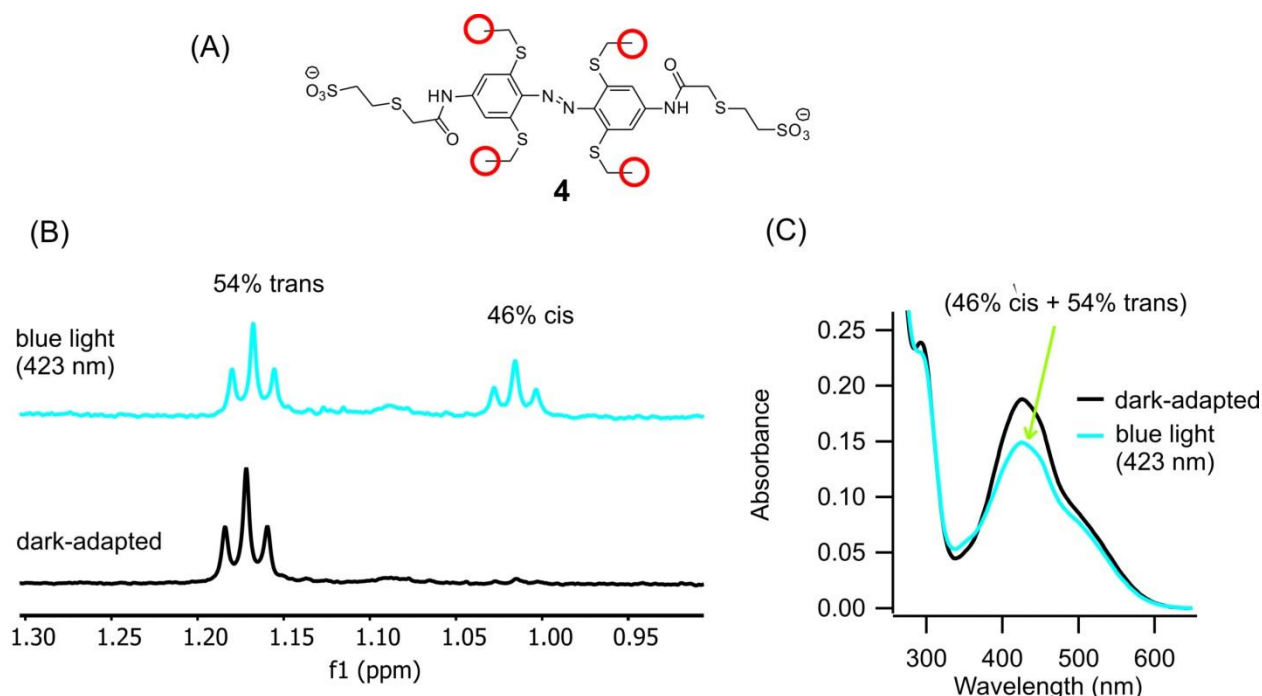


Figure S8. (A) Structure of compound (**4**). (B) Expanded ¹H NMR spectra showing methyl proton signals (highlighted with red circles) of (**4**) in 0.6 mM phosphate buffer (pH 7); dark-adapted spectrum (black line) and after irradiation with 423 nm light (blue lines). (C) UV/Vis absorption spectra of dark-adapted state (black line) and after irradiation with 423 nm light (blue line) acquired under the same conditions as for ¹H NMR acquisition.

6) Glutathione stability of (4): A 33 μM solution of (**4**) in 100 mM sodium phosphate buffer, pH 7 was mixed with 0.25 M glutathione (prepared by dissolving solid reduced glutathione in 0.5 M sodium phosphate buffer and adjusting the pH to 7 by adding NaOH solution) to give a final concentration of 10 mM reduced glutathione (GSH). To suppress GSH self-oxidation, the resulting solution was supplemented with 5 mM TCEP (triscarboxyethyl phosphine). During the incubation of the resulting solution at 25°C for 16 h, UV/Vis absorption spectra were acquired

at 1h intervals in a Perkin-Elmer Lambda 25 spectrophotometer, no reduction of the absorption intensity was noticed (Fig. S9) suggesting that the compound (**4**) would be stable and functional intracellularly.

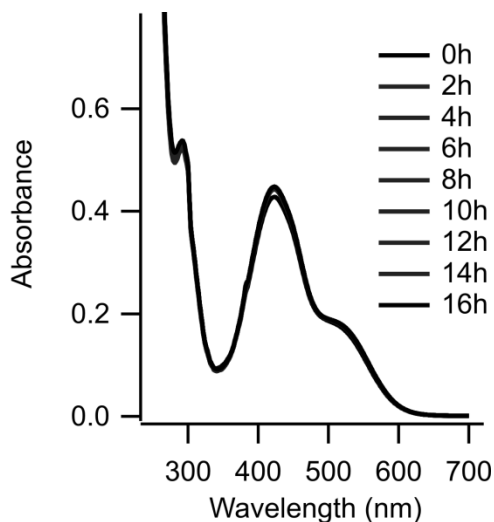


Fig. S9: UV/Vis absorption spectra of a solution of (**4**) incubated with 10 mM GSH at 25°C; scans were acquired at 1h intervals (shown 2h) over a period of 16h.

UV/Vis absorption spectra and thermal cis-to-trans relaxation rate of (5**):** Ultraviolet absorbance spectra and thermal relaxation rates of the isomers in various solvents were obtained using a diode array UV–Vis spectrophotometer (Ocean Optics Inc., USB4000) coupled to a temperature controlled cuvette holder (Quantum Northwest, Inc.) (Fig. S9) as mentioned above. Inefficient switching of (**5**) in aqueous buffer upon exposed to blue (423 nm) or violet (407 nm) light (Fig S9A) signifies a lack of thermal stability of its cis isomer (Fig S10). A 39-fold decrease in the thermal relaxation rate in DMSO led to significant switching even at 25°C (Fig. S10). Multiple rounds of photoswitching in aqueous buffer without any noticeable change in absorption intensity indicate lack of photobleaching (Fig. S11).

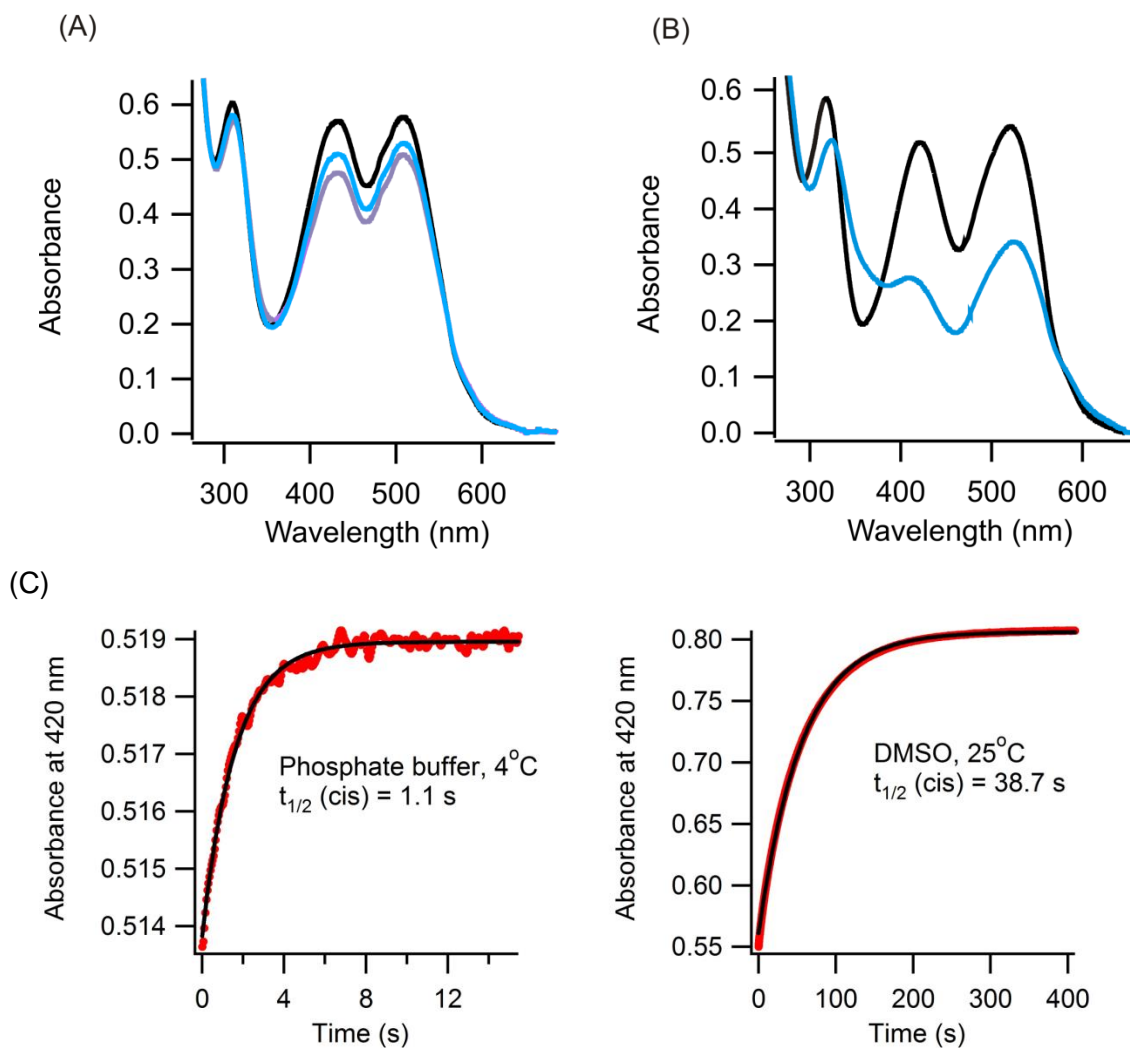


Fig. S9. UV-Vis absorption spectra of (**5**) in 1 mM phosphate buffer (pH 7) at 4°C (A) and in DMSO at 25°C (B): dark-adapted spectra (black lines), steady state spectra under blue light (423nm)(blue lines) and violet light (407 nm)(violet lines) illumination. (C) Thermal cis-to-trans relaxation of (**5**) under various conditions (indicated); black lines represent mono-exponential fits of the experimental data (red lines).

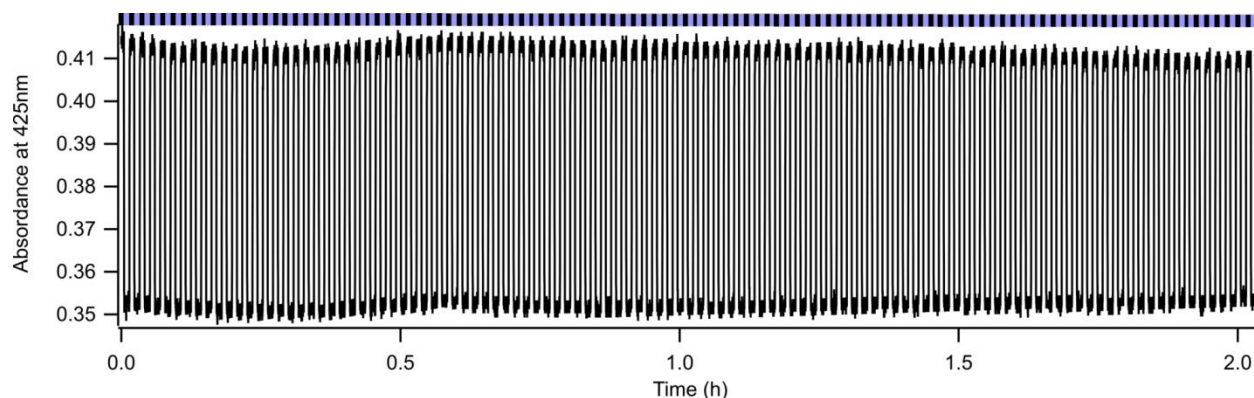


Fig. S11. Multiple rounds of photoswitching of **(5)** in 1 mM phosphate buffer (pH 7) upon intermittent exposure to violet light (407 nm) at 4°C.

Glutathione stability of (5): A 27 μM solution of **(5)** was incubated with 10 mM reduced glutathione (GSH) supplemented with 5 mM TCEP in 100 mM phosphate buffer (pH 7) as described above. During incubation at 25°C for 17 h, UV/Vis absorption spectra were acquired at 1h intervals (shown 2h intervals) using a Perkin-Elmer Lambda 25 spectrophotometer. No reduction of the absorption intensity was noticed (Fig. S12). After incubation for 20h, the sample underwent photoswitching normally upon illumination with violet light (Fig S12).

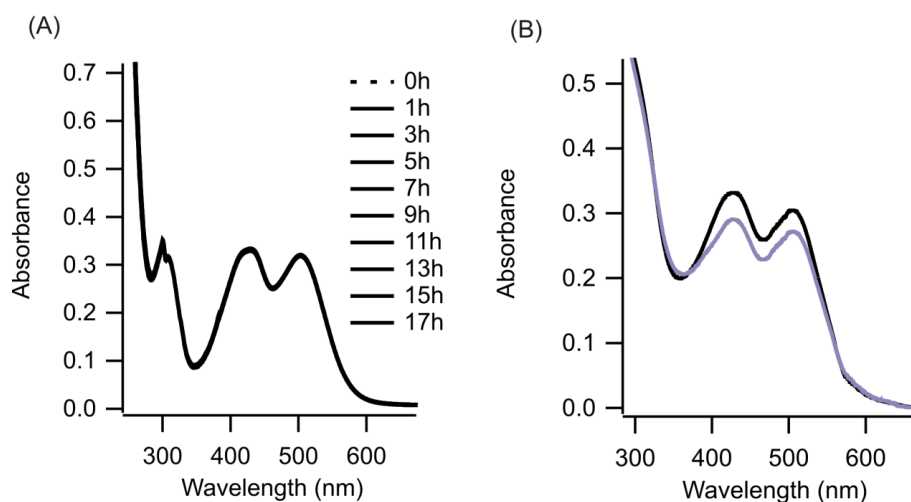


Fig. S12: (A) UV/Vis absorption spectra of a solution of **(5)** incubated with 10 mM GSH at 25°C; scans were acquired at 1h intervals (shown 2h) over a period of 17h. (B) Photoswitching of **(5)** with violet light after 20 h of incubation with 10mM GSH at 25°C.

7) Computational Chemistry:

The geometries of the cis and trans forms of **1**, **2'** and **3'** were calculated with the nonlocal hybrid Becke three-parameter Lee-Yang-Parr (B3LYP) functional¹ and the 6-311++g(d,p) basis set with a DMSO solvent model (SCRF)² using the Gaussian 09 suit of programs.³ The first six singlet excited-states were calculated with TD-DFT⁴ using the optimized geometries with the DMSO solvent model. The calculated UV-Vis spectra shown were generated from the TD-DFT data with Gaussview⁵ by applying a Gaussian function with 0.2 eV peak half width at half height on each transition.

Graphical images of bond density surfaces ($0.1 e/au^3$) colored by |HOMO|, |LUMO| etc. were generated using Spartan 09 Software.⁶

Ground state free energies (sum of electronic and thermal energies) of trans and cis isomers of **1**, **2'**, and **3'** were calculated from a frequency calculation and are shown in Table SI1.

Table SI1. Free energies for **1**, **2'** and **3'**

Compound	Trans energy G°(eV)	Cis energy (eV) G°(eV)	Difference (Trans-cis) G°(eV)
1	-39373.33	-39372.99	-0.33 (7.70 kcal/mol)
2'	-66220.23	-66219.47	-0.75 (17.14 kcal/mol)
3'	-74529.15	-74528.43	-0.73 (16.73 kcal/mol)

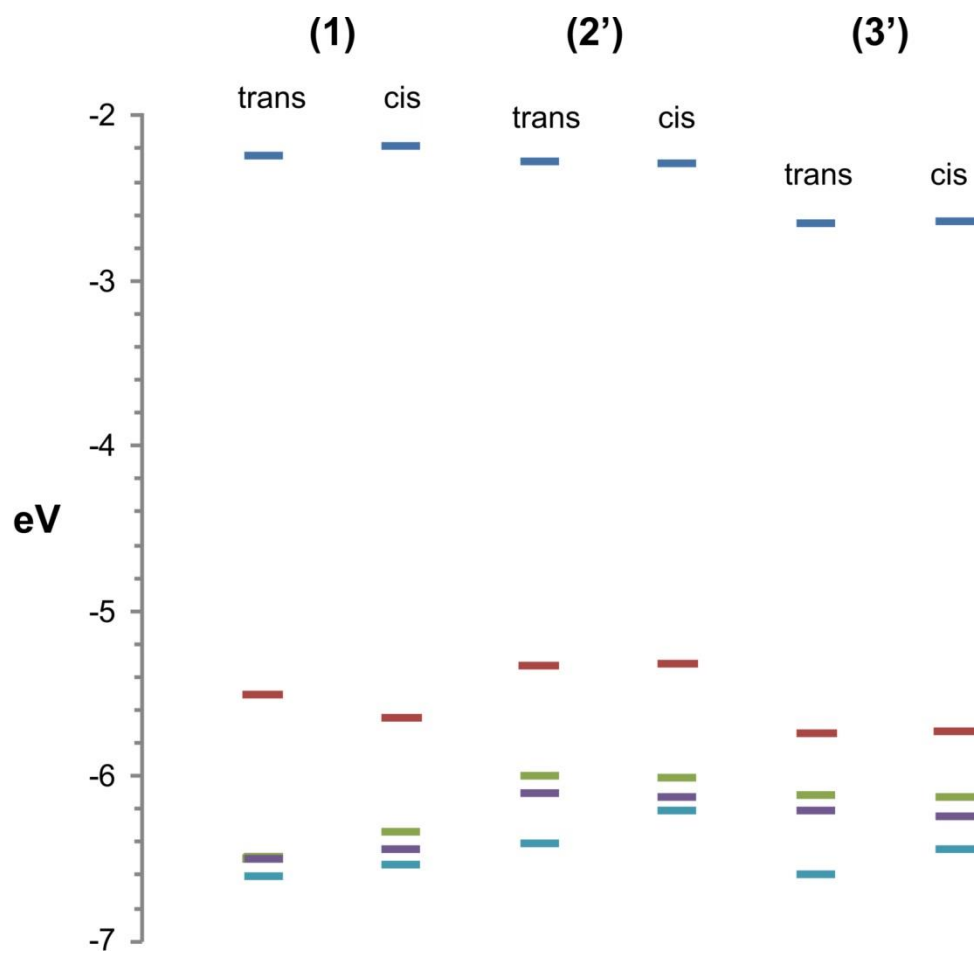


Fig. S13: Calculated orbital energies of trans and cis isomers of compounds **1**, **2'** and **3'** in eV.

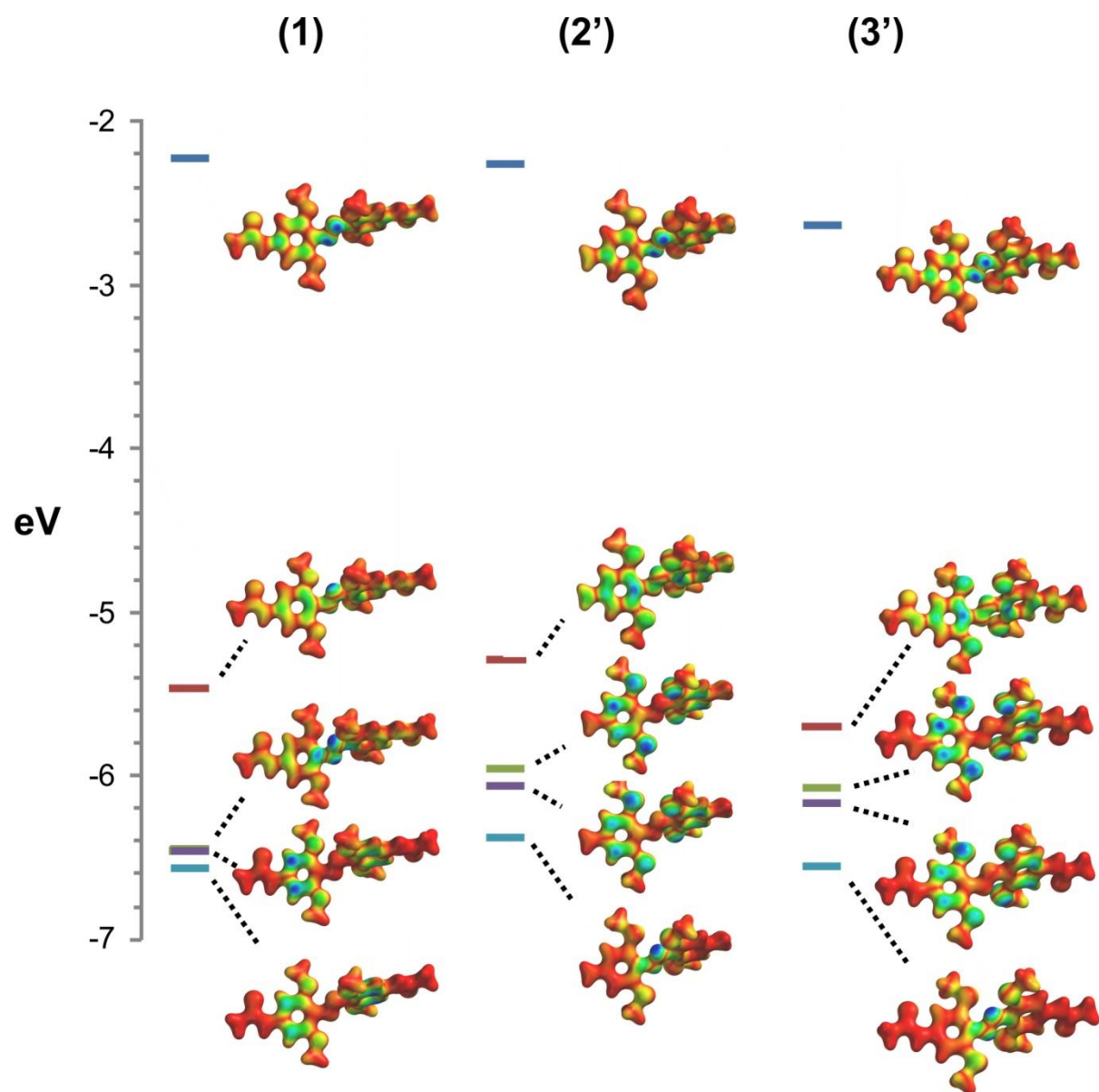


Fig. S14: Electron density surfaces for the trans isomers of **1**, **2'** and **3'** with the |LUMO|, |HOMO|, |HOMO-1|, |HOMO-2| and |HOMO-3| color mapped from highest (blue) to lowest (red).

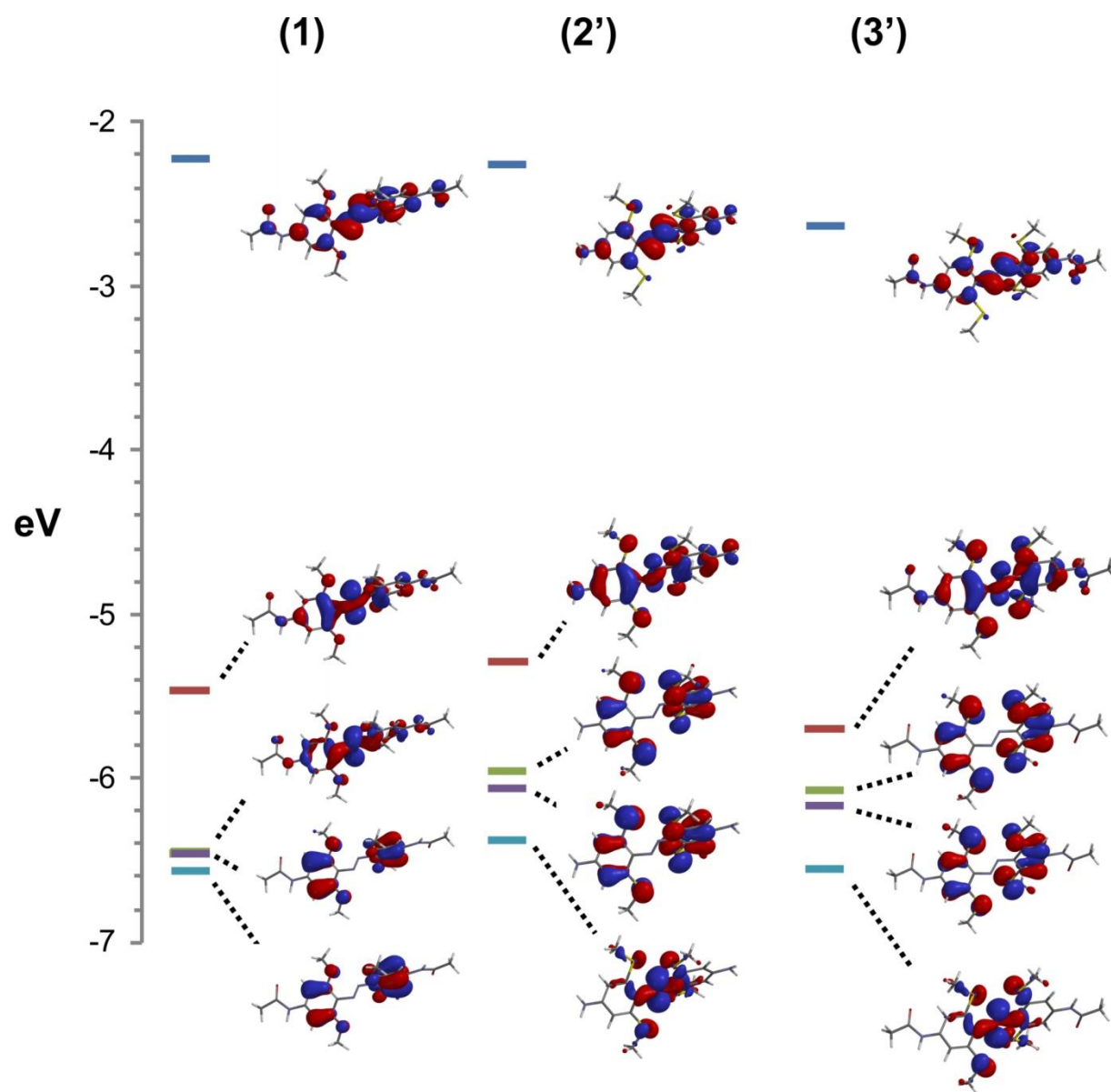


Fig. S15: Calculated orbital diagrams for the trans isomers of **1**, **2'** and **3'**.

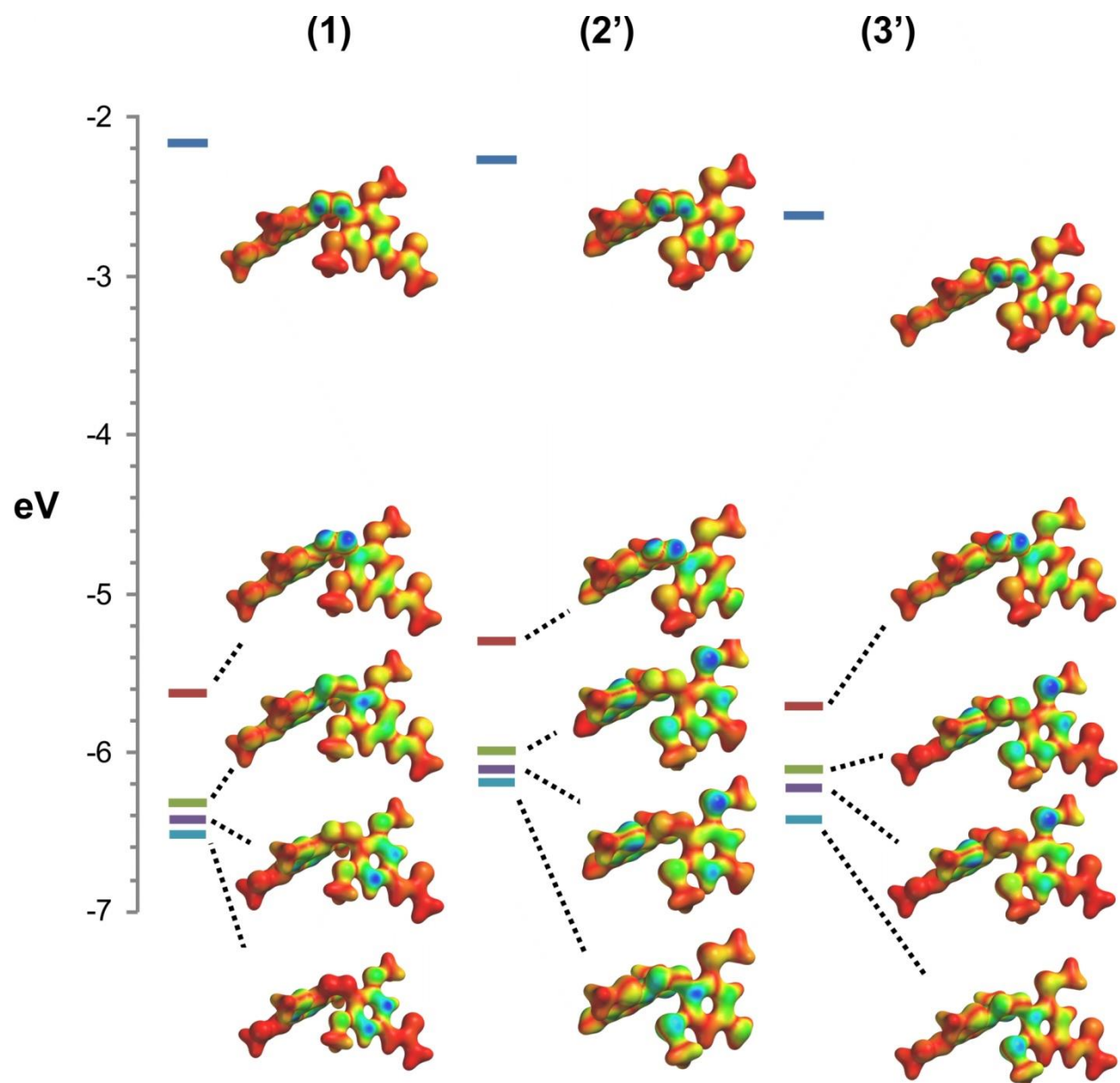


Fig. S16: Electron density surfaces for the cis isomers of **1**, **2'** and **3'** with the $|LUMO|$, $|HOMO|$, $|HOMO-1|$, $|HOMO-2|$ and $|HOMO-3|$ color mapped from highest (blue) to lowest (red).

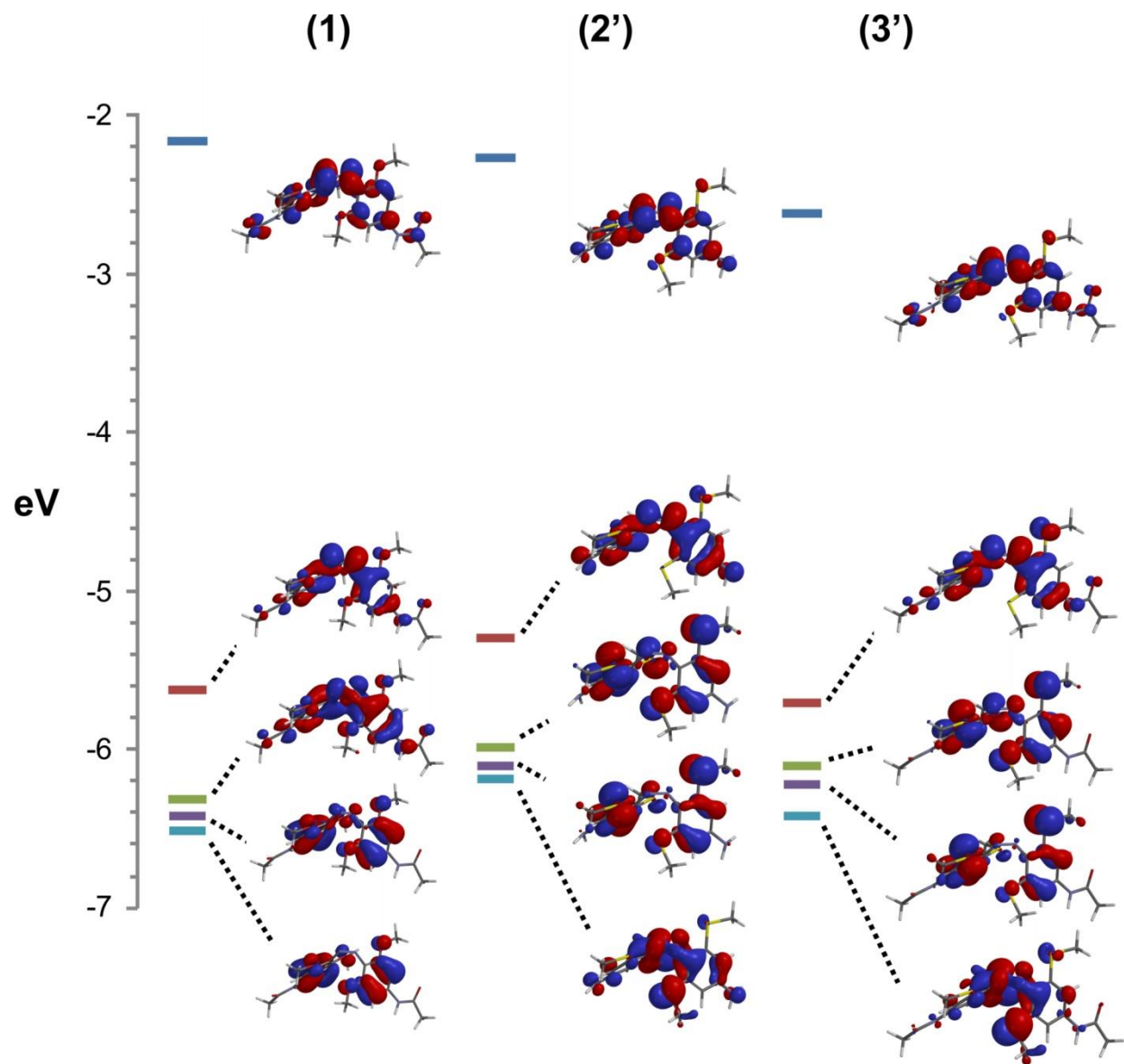


Fig. S17: Calculated orbital diagrams for the cis isomers of **1**, **2'** and **3'**.

Computational details:

Contribution of each orbital to the transition is calculated by

$$\%=(2*(c^2))*100$$

Where c is the orbital coefficient

(1)-trans: Optimized geometry and first 20 excited states

C	-1.97574	-1.47501	-2.0666
C	-1.0912	-1.50019	-0.99413
C	-0.49224	-0.3093	-0.50683
C	-0.79809	0.90474	-1.17374
C	-1.67247	0.92717	-2.26503
C	-2.26591	-0.25892	-2.70013
H	-2.44775	-2.38305	-2.4142
H	-1.90018	1.84499	-2.77695
N	0.46871	-0.46893	0.50567
N	0.54969	0.45954	1.35366
C	1.59493	0.37172	2.28773
C	2.91622	-0.06762	2.01658
C	1.33037	0.91684	3.5716
C	3.91969	0.02472	2.98657
C	2.32277	0.98939	4.54255
C	3.61809	0.54308	4.24695
H	4.92449	-0.29799	2.78024
H	2.10567	1.38295	5.52536
C	-0.2666	3.22272	-1.51861
H	-1.29135	3.60318	-1.52243
H	0.3836	3.94167	-1.0243
H	0.07371	3.06375	-2.54533
C	-1.29038	-3.88486	-0.79496
H	-0.98116	-4.08155	-1.82507
H	-0.86813	-4.64168	-0.13726
H	-2.38123	-3.90828	-0.72335
C	4.52855	-0.7777	0.38298
H	4.4844	-1.05218	-0.669
H	5.15088	0.11271	0.50551
H	4.95041	-1.6067	0.95712
C	-0.2737	1.95004	5.03041
H	0.32908	2.84779	5.19238
H	-1.32301	2.22593	4.94978
H	-0.14308	1.25842	5.86726
N	-3.1728	-0.31188	-3.77606
H	-3.52031	-1.23551	-3.9898
N	4.57055	0.64997	5.27855
H	4.21454	1.02708	6.14493
C	5.90679	0.33502	5.27646

C	-3.64965	0.69879	-4.5734
O	6.49511	-0.12702	4.30419
O	-3.32673	1.87539	-4.44564
C	6.6231	0.59695	6.58495
H	5.99474	1.06052	7.34573
H	7.00387	-0.35204	6.96948
H	7.48115	1.24279	6.3885
C	-4.61809	0.25612	-5.65048
H	-4.17904	0.47916	-6.62572
H	-4.86863	-0.80411	-5.60979
H	-5.5337	0.84332	-5.55769
O	-0.76868	-2.63739	-0.32787
O	-0.16192	2.0224	-0.74604
O	0.05431	1.32483	3.78623
O	3.17354	-0.51983	0.7654

1-trans

Excited State	Energy	Oscillator Strength (f)	Orbitals and coefficients (110=HOMO, 111=LUMO)
1	2.3157 eV 535.42 nm	0.2874	107 ->111 -0.24622 110 ->111 0.65407
2	3.4373 eV 360.70 nm	0.8499	107 ->111 0.64155 108 ->111 0.10307 110 ->111 0.25697
3	3.5588 eV 348.39 nm	0.0258	109 ->111 0.69420 110 ->117 0.10027
4	3.5650 eV 347.78 nm	0.0369	107 ->111 -0.10443 108 ->111 0.68642 110 ->116 -0.10318
5	3.8693 eV 320.43 nm	0.0009	106 ->111 0.59171 110 ->112 -0.36891
6	4.2651 eV 290.70 nm	0.0174	106 ->111 0.35206 110 ->112 0.57180 110 ->113 -0.11363
7	4.5466 eV 272.70 nm	0.1140	110 ->114 0.65355 110 ->115 -0.17755
8	4.5841 eV 270.47 nm	0.0001	110 ->113 0.65877 110 ->118 -0.15157
9	4.6590 eV 266.12 nm	0.0476	109 ->112 0.24135 110 ->116 0.63107
10	4.6693 eV 265.53 nm	0.0271	105 ->111 0.13374 108 ->112 -0.23523 110 ->117 0.61144
11	4.7045 eV 263.55 nm	0.0020	104 ->112 0.18461 105 ->111 0.63966 105 ->114 -0.10906 110 ->117 -0.11526
12	4.7120 eV 263.12 nm	0.0007	104 ->111 0.63609

Excited State	Energy	Oscillator Strength (f)	Orbitals and coefficients (110=HOMO, 111=LUMO)
			104 ->114 -0.10571
			105 ->112 0.18894
			110 ->114 -0.11891
			110 ->115 -0.12022
13	4.7451 eV 261.29 nm	0.0039	104 ->111 0.14151
			110 ->114 0.16538
			110 ->115 0.65590
14	4.9433 eV 250.81 nm	0.0000	110 ->113 0.17363
			110 ->118 0.64567
15	4.9774 eV 249.10 nm	0.0771	103 ->111 0.69055
16	5.0016 eV 247.89 nm	0.0008	109 ->112 -0.10253
			110 ->119 0.67569
17	5.0289 eV 246.54 nm	0.0034	102 ->111 0.69295
18	5.0787 eV 244.13 nm	0.0001	108 ->112 -0.13286
			110 ->120 0.65975
			110 ->122 -0.12368
19	5.1070 eV 242.77 nm	0.0011	107 ->112 0.53372
			107 ->117 -0.10924
			108 ->112 0.34836
			110 ->117 0.10386
			110 ->120 0.14247
20	5.1268 eV 241.84 nm	0.0779	106 ->117 0.14172
			107 ->116 0.20287
			108 ->114 0.11823
			109 ->112 0.57934
			110 ->116 -0.22577
			110 ->119 0.13105

(1)-cis: Optimized geometry and first 20 excited states

C	0.53292	-3.99546	1.54039
C	0.9096	-2.72371	1.11016
C	-0.04897	-1.6914	1.00346
C	-1.39662	-2.00346	1.28277
C	-1.77813	-3.26898	1.72919
C	-0.80352	-4.2625	1.86103
H	1.26747	-4.78479	1.61913
H	-2.79989	-3.49546	1.97668
N	0.2089	-0.43201	0.40001
N	1.15188	0.33011	0.71573
C	1.96939	0.16945	1.86591
C	3.3542	0.38507	1.70228
C	1.46382	0.05411	3.18005
C	4.22569	0.41078	2.79124
C	2.32723	0.09361	4.27441
C	3.70389	0.25837	4.07925
H	5.28541	0.54034	2.6616

H	1.9386	0.00844	5.27969
C	-3.67036	-1.23312	1.32562
H	-3.873	-1.51101	2.36338
H	-4.1715	-0.29495	1.09638
H	-4.03312	-2.01652	0.65489
C	3.17068	-3.44097	0.72017
H	2.89441	-4.26335	0.05464
H	4.07637	-2.96339	0.35296
H	3.34358	-3.82162	1.73037
C	5.14905	0.83015	0.16966
H	5.22875	0.95435	-0.90837
H	5.44593	1.75632	0.66884
H	5.79908	0.01182	0.49076
C	-0.46673	-0.04104	4.60895
H	-0.2121	0.8685	5.15989
H	-1.54176	-0.08066	4.44777
H	-0.15111	-0.92037	5.17678
N	-1.09694	-5.56821	2.30365
H	-0.30171	-6.18888	2.34531
N	4.50785	0.26639	5.23711
H	4.00362	0.13165	6.10142
C	5.86403	0.43111	5.36185
C	-2.2939	-6.11631	2.6892
O	6.61819	0.60852	4.41
O	-3.35424	-5.49836	2.69893
C	6.38497	0.3791	6.78341
H	5.61087	0.21061	7.53235
H	7.12669	-0.4195	6.85253
H	6.89201	1.32138	7.00213
C	-2.22003	-7.56795	3.11591
H	-2.9244	-8.14416	2.5126
H	-1.22624	-8.00568	3.01881
H	-2.53953	-7.64112	4.15797
O	0.116	-0.03295	3.30295
O	3.77328	0.52603	0.41919
O	-2.27653	-0.98259	1.12227
O	2.17135	-2.41804	0.71863

(2')-trans: Optimized geometry and first 20 excited states

C	-2.465	-1.30976	-1.78854
C	-1.46142	-1.31462	-0.83218
C	-0.94304	-0.09565	-0.31171
C	-1.44491	1.1346	-0.82329
C	-2.44519	1.11596	-1.79452
C	-2.96666	-0.09153	-2.27969
H	-2.87742	-2.23263	-2.17201
H	-2.83862	2.04004	-2.19472
N	0.07743	-0.23261	0.62466
N	0.23721	0.73094	1.43233
C	1.34261	0.66571	2.27466
C	2.5619	-0.01757	2.00159
C	1.2362	1.41964	3.47751
C	3.60665	0.05085	2.92256
C	2.28296	1.46262	4.38507
C	3.48126	0.77884	4.11413
H	4.54057	-0.45949	2.73254
H	2.20027	2.01819	5.30863
S	-0.78768	-2.82005	-0.15065
S	-0.74842	2.68684	-0.27812
S	-0.31948	2.24686	3.76408
S	2.7744	-0.89713	0.46164
C	-1.1603	3.81332	-1.66372
H	-2.22162	4.05882	-1.69441
H	-0.59875	4.72399	-1.45123
H	-0.83463	3.40437	-2.62012
C	-1.65224	-4.12512	-1.08755
H	-1.44781	-4.05582	-2.15602
H	-1.2376	-5.05927	-0.70768
H	-2.72609	-4.11348	-0.90095
C	4.59732	-0.9553	0.28454
H	4.76065	-1.33326	-0.72555
H	5.0387	0.03736	0.37304
H	5.05909	-1.64359	0.99216
C	-0.04195	3.11757	5.34312
H	0.77346	3.83689	5.26703
H	-0.97192	3.655	5.5304
H	0.13557	2.42193	6.16334
N	-3.92738	-0.0876	-3.27556
H	-4.48383	-0.924	-3.37639
H	-4.4625	0.76082	-3.39048
N	4.54685	0.87204	4.99153
H	4.33401	1.13093	5.94395
H	5.25961	0.16024	4.9228

2'-trans

Excited State	Energy	Oscillator Strength (f)	Orbitals and coefficients (104=HOMO, 105=LUMO)
1	2.4066 eV 515.19 nm	0.3593	99 ->105 -0.11681
			101 ->105 -0.23954
			104 ->105 0.65014
2	3.0195 eV 410.61 nm	0.0220	103 ->105 0.70092
			101 ->105 0.65394
3	3.0441 eV 407.29 nm	0.2889	104 ->105 0.25228
			102 ->105 0.69599
4	3.1393 eV 394.94 nm	0.0784	98 ->105 0.34417
			100 ->105 0.58585
			104 ->106 0.12090
			104 ->111 0.10839
6	3.8407 eV 322.82 nm	0.2136	99 ->105 0.68905
			98 ->105 0.60851
7	3.8965 eV 318.19 nm	0.0002	100 ->105 -0.32829
			100 ->105 -0.10962
8	4.0516 eV 306.02 nm	0.0615	104 ->106 0.67695
			104 ->107 0.67989
9	4.1016 eV 302.28 nm	0.1949	104 ->108 0.69439
			104 ->109 0.69142
10	4.3858 eV 282.69 nm	0.0001	102 ->106 -0.22496
			103 ->107 -0.24218
11	4.4964 eV 275.74 nm	0.0192	104 ->111 0.58660
			104 ->110 0.68379
12	4.6780 eV 265.04 nm	0.0020	103 ->107 0.14295
			104 ->112 0.65925
13	4.6836 eV 264.72 nm	0.0033	103 ->106 0.65076
			104 ->114 0.20088
14	4.7824 eV 259.25 nm	0.0008	100 ->107 -0.11213
			101 ->106 0.30829
15	4.7989 eV 258.36 nm	0.1506	102 ->106 -0.29192
			103 ->107 0.52625
16	4.8459 eV 255.85 nm	0.0024	104 ->112 -0.10097
			101 ->106 -0.22252
17	4.8720 eV 254.48 nm	0.0069	102 ->106 0.20481
			103 ->107 0.16703
18	4.8865 eV 253.73 nm	0.0330	104 ->111 0.13330
			104 ->113 0.56758
19	4.9112 eV 252.45 nm	0.2676	104 ->115 0.10479
			100 ->106 0.11707
			101 ->107 -0.33591
			102 ->107 0.46370
			103 ->106 -0.10280
			103 ->108 -0.12702
			104 ->114 0.32162
			101 ->107 0.34864
			102 ->107 -0.11659
			103 ->106 -0.19498
			103 ->108 0.11455
			104 ->114 0.52571

Excited State	Energy	Oscillator Strength (f)	Orbitals and coefficients (104=HOMO, 105=LUMO)
20	4.9351 eV 251.23 nm	0.0005	101 ->106 0.55653 102 ->106 0.22998 103 ->107 -0.21872 104 ->113 0.22367

(2')-cis: Optimized geometry and first 20 excited states

C	0.1708	-3.83128	1.77098
C	0.58251	-2.53941	1.44367
C	-0.37422	-1.48708	1.38896
C	-1.74857	-1.82395	1.5653
C	-2.13403	-3.1098	1.9108
C	-1.17356	-4.12807	2.02762
H	0.89152	-4.63586	1.8197
H	-3.17343	-3.35421	2.08069
N	-0.16424	-0.17636	0.92319
N	0.80149	0.59508	1.17699
C	1.7699	0.46988	2.18935
C	3.04953	0.98726	1.83097
C	1.54282	0.14024	3.55513
C	4.08419	1.04504	2.75163
C	2.59223	0.22406	4.47001
C	3.86816	0.65241	4.08289
H	5.06429	1.40289	2.46785
H	2.43	-0.03178	5.50806
S	2.27837	-2.23559	0.98034
S	-2.91668	-0.49322	1.36329
S	-0.10159	-0.25797	4.1225
S	3.24237	1.50192	0.13592
C	-4.53206	-1.32282	1.54319
H	-4.67089	-1.72309	2.54743
H	-5.26829	-0.53731	1.37119
H	-4.66579	-2.10545	0.79633
C	2.86542	-3.8791	0.43719
H	2.1892	-4.3121	-0.29922
H	3.83264	-3.68503	-0.02765
H	3.01005	-4.55985	1.27514
C	4.9226	2.21337	0.10239
H	5.04214	2.59495	-0.91191
H	5.02093	3.03922	0.80696
H	5.68621	1.45805	0.2876
C	-0.05572	0.20525	5.89003
H	0.31723	1.2209	6.01754
H	-1.09587	0.15658	6.21378
H	0.52873	-0.49713	6.48277

N	-1.56352	-5.42578	2.31756
H	-0.84967	-6.04394	2.67559
H	-2.45086	-5.53746	2.78657
N	4.88596	0.7619	5.01673
H	4.78877	0.21407	5.85947
H	5.8299	0.76674	4.65819

2'-cis

Excited State	Energy	Oscillator Strength (f)	Orbitals and coefficients (104=HOMO, 105=LUMO)
1	2.2263 eV 556.90 nm	0.1846	99 ->105 0.16449 104 ->105 0.67745
2	2.9848 eV 415.39 nm	0.0687	103 ->105 0.69314
3	3.0989 eV 400.09 nm	0.0110	102 ->105 0.70088
4	3.2995 eV 375.76 nm	0.0210	100 ->105 0.13534 101 ->105 0.66911 104 ->107 -0.12365
5	3.3882 eV 365.93 nm	0.1961	99 ->105 0.67207 104 ->105 -0.16736
6	3.7479 eV 330.81 nm	0.0293	100 ->105 0.67861 101 ->105 -0.10111 104 ->107 0.12868
7	3.8651 eV 320.78 nm	0.0977	98 ->105 -0.14853 104 ->106 0.67255
8	3.9478 eV 314.06 nm	0.0840	98 ->105 0.67510 104 ->106 0.14301
9	3.9804 eV 311.49 nm	0.0854	101 ->105 0.11743 104 ->107 0.66015 104 ->109 -0.10628
10	4.3525 eV 284.86 nm	0.0051	104 ->108 0.69645
11	4.4430 eV 279.06 nm	0.0028	102 ->106 0.11794 103 ->107 0.19903 104 ->109 0.63064
12	4.5121 eV 274.78 nm	0.0003	104 ->110 0.68268
13	4.5376 eV 273.24 nm	0.0547	103 ->106 -0.23746 104 ->111 0.62663 104 ->114 -0.15110
14	4.6199 eV 268.37 nm	0.0065	101 ->106 0.48718 102 ->106 -0.18421 103 ->107 0.41305 104 ->109 -0.15682
15	4.6674 eV 265.64 nm	0.0710	102 ->107 -0.21847 103 ->106 0.61426 104 ->111 0.23027
16	4.7193 eV 262.72 nm	0.0001	101 ->106 -0.36997 102 ->106 0.14279 103 ->107 0.46519 104 ->112 0.30061
17	4.7519 eV 260.92 nm	0.0523	101 ->107 0.59548 102 ->107 0.18196 102 ->109 0.16164

Excited State	Energy	Oscillator Strength (f)	Orbitals and coefficients (104=HOMO, 105=LUMO)
18	4.7588 eV 260.54 nm	0.0237	103 ->106 0.13504
			101 ->106 0.28119
			101 ->107 -0.11007
			102 ->106 0.47264
			103 ->107 -0.16885
19	4.8131 eV 257.60 nm	0.2148	104 ->112 0.37118
			101 ->107 -0.24507
			102 ->107 0.58941
			103 ->106 0.15087
			103 ->108 0.11100
20	4.8423 eV 256.04 nm	0.0572	100 ->106 0.11044
			102 ->106 -0.39282
			103 ->109 -0.20377
			104 ->109 0.17604
			104 ->112 0.45413

(3')-trans: Optimized geometry and first 20 excited states

C	-1.84033	-1.51804	-2.1227
C	-0.94008	-1.53878	-1.06962
C	-0.48404	-0.32131	-0.49227
C	-0.93765	0.91222	-1.03051
C	-1.83209	0.91055	-2.10703
C	-2.28577	-0.29379	-2.64699
H	-2.21014	-2.43733	-2.55535
H	-2.1891	1.83018	-2.5347
N	0.45681	-0.46434	0.52607
N	0.52741	0.47943	1.36454
C	1.56824	0.41122	2.28927
C	2.82557	-0.21244	2.07243
C	1.34218	1.10986	3.50763
C	3.81132	-0.14549	3.0636
C	2.32622	1.15034	4.48256
C	3.56439	0.5255	4.26232
H	4.77173	-0.60836	2.92491
H	2.15733	1.66047	5.42087
S	-0.33621	-3.04914	-0.34119
S	-0.3282	2.4582	-0.38385
S	-0.25865	1.86512	3.71531
S	3.17772	-1.02057	0.52182
C	-0.60212	3.61067	-1.78071
H	-1.65773	3.84038	-1.92249
H	-0.08203	4.52301	-1.48605
H	-0.16572	3.22837	-2.70314
C	-1.09293	-4.343	-1.38075
H	-0.7819	-4.25392	-2.42163
H	-0.71048	-5.2803	-0.97603

H	-2.18001	-4.3415	-1.30125
C	5.0082	-0.99198	0.46517
H	5.25398	-1.31689	-0.5466
H	5.39541	0.01395	0.62535
H	5.45132	-1.69061	1.1741
C	-0.12589	2.67835	5.34234
H	0.66307	3.43041	5.352
H	-1.08753	3.17242	5.48292
H	0.02024	1.95518	6.1446
N	-3.19495	-0.36386	-3.71802
H	-3.445	-1.30103	-3.9993
N	4.50936	0.61915	5.30018
H	4.20097	1.13967	6.10885
C	5.77992	0.10129	5.38077
C	-3.79246	0.6474	-4.43145
O	6.30278	-0.55443	4.48654
O	-3.59166	1.83776	-4.21755
C	6.5053	0.39705	6.67647
H	5.93739	1.02126	7.36651
H	6.74058	-0.55043	7.16649
H	7.44971	0.89195	6.44138
C	-4.7387	0.18504	-5.51935
H	-4.42086	0.62447	-6.4669
H	-4.79046	-0.89841	-5.62777
H	-5.73732	0.56705	-5.29543

3'-trans

Excited State	Energy	Oscillator Strength (f)	Orbitals and coefficients (126=HOMO, 127=LUMO)
1	2.3358 eV 530.81 nm	0.3166	121 ->127 -0.11115
			123 ->127 0.25953
			126 ->127 0.64217
2	2.7900 eV 444.39 nm	0.0257	125 ->127 0.70261
			3
124 ->127 0.52084			
126 ->127 -0.16098			
4	2.9207 eV 424.49 nm	0.2723	123 ->127 0.47072
			124 ->127 -0.46775
			126 ->127 -0.22566
5	3.5139 eV 352.84 nm	0.0054	120 ->127 -0.13621
			122 ->127 0.68050
6	3.8274 eV 323.94 nm	0.4450	121 ->127 0.68863
			7
122 ->127 0.10102			
126 ->128 0.17155			
124 ->128 -0.20012			
8	4.2563 eV 291.29 nm	0.0403	126 ->128 -0.29867
			126 ->129 0.58425

Excited State	Energy	Oscillator Strength (f)	Orbitals and coefficients (126=HOMO, 127=LUMO)
9	4.2928 eV 288.82 nm	0.1170	125 ->128 0.27218
			126 ->130 0.62183
10	4.3557 eV 284.65 nm	0.0044	119 ->127 0.45775
			126 ->128 0.44338
			126 ->129 0.19659
11	4.3889 eV 282.49 nm	0.0010	118 ->127 0.68262
			119 ->128 0.13131
12	4.3940 eV 282.17 nm	0.0026	119 ->127 0.50792
			120 ->127 0.11008
			126 ->128 -0.38621
			126 ->129 -0.17284
13	4.6819 eV 264.82 nm	0.1148	125 ->128 0.42823
			126 ->130 -0.22685
			126 ->131 0.47611
14	4.6978 eV 263.92 nm	0.1854	123 ->130 0.10991
			125 ->128 -0.42121
			126 ->130 0.17552
			126 ->131 0.48913
15	4.7434 eV 261.38 nm	0.0534	123 ->129 0.11876
			124 ->128 0.60763
			125 ->130 -0.13380
			125 ->131 -0.13331
			126 ->129 0.22828
16	4.7786 eV 259.46 nm	0.0027	125 ->130 -0.13834
			126 ->132 0.65639
			126 ->135 0.11403
17	4.7961 eV 258.51 nm	0.3429	125 ->128 -0.14442
			125 ->129 0.67528
18	4.8406 eV 256.14 nm	0.0145	124 ->128 0.12667
			124 ->129 0.13750
			125 ->130 0.64839
			126 ->132 0.12160
19	4.8912 eV 253.48 nm	0.2740	123 ->130 -0.19914
			124 ->129 -0.17179
			124 ->130 0.61030
			126 ->133 0.15519
20	4.8951 eV 253.28 nm	0.0178	123 ->128 0.13002
			123 ->129 -0.13234
			124 ->129 0.61345
			124 ->130 0.17270

(3')-cis: Optimized geometry and first 20 excited states

C	0.28628	-3.94386	1.36977
C	0.75673	-2.64165	1.20783
C	-0.16848	-1.56154	1.24632
C	-1.55576	-1.86273	1.34452
C	-2.00323	-3.16713	1.52309
C	-1.07483	-4.2137	1.54306
H	0.97955	-4.77371	1.35409
H	-3.04781	-3.39572	1.63673
N	0.10092	-0.21426	0.93902
N	1.07444	0.48885	1.31217
C	1.9991	0.21909	2.33871
C	3.30888	0.70963	2.07734
C	1.69839	-0.24052	3.6507
C	4.3161	0.62925	3.03265
C	2.7176	-0.29644	4.60016
C	4.02025	0.11379	4.29944
H	5.31838	0.96061	2.82716
H	2.50579	-0.65774	5.59718
S	2.47617	-2.34938	0.84452
S	-2.67294	-0.47961	1.27137
S	0.02207	-0.63042	4.11207
S	3.59168	1.38131	0.45419
C	-4.31851	-1.26813	1.27471
H	-4.51604	-1.78464	2.21363
H	-5.02083	-0.44071	1.17085
H	-4.4381	-1.94613	0.42993
C	3.0324	-3.94097	0.13938
H	2.37275	-4.26285	-0.66561
H	4.02271	-3.72933	-0.26478
H	3.12254	-4.7152	0.90011
C	5.29186	2.03521	0.56091
H	5.46674	2.50846	-0.40558
H	5.38208	2.78465	1.34693
H	6.02209	1.23901	0.70266
C	0.01364	-0.35745	5.91891
H	0.41814	0.62341	6.1662
H	-1.03983	-0.39678	6.19717
H	0.54677	-1.14295	6.45272
N	-1.43581	-5.56259	1.71519
H	-0.66241	-6.21172	1.70013
N	4.9762	-0.0059	5.32496
H	4.61972	-0.37049	6.19671
C	6.31996	0.27877	5.30771
C	-2.67621	-6.1216	1.90424
O	6.90574	0.72674	4.3279

O	-3.71402	-5.46967	1.94621
C	7.04563	-0.00103	6.60688
H	6.40882	-0.42105	7.38561
H	7.86508	-0.69374	6.40433
H	7.48276	0.93197	6.96938
C	-2.67898	-7.62806	2.05932
H	-3.31049	-8.056	1.27781
H	-1.68866	-8.08049	2.0029
H	-3.12965	-7.8772	3.0224

3'-cis

Excited State	Energy	Oscillator Strength (f)	Orbitals and coefficients (126=HOMO, 127=LUMO)
1	2.2281 eV 556.45 nm	0.2048	120 ->127 0.10857 122 ->127 -0.14698 125 ->127 -0.10837 126 ->127 0.66959
2	2.7791 eV 446.13 nm	0.0790	125 ->127 0.68591 126 ->127 0.13012
3	2.9031 eV 427.07 nm	0.0164	124 ->127 0.70218
4	3.1625 eV 392.05 nm	0.0073	123 ->127 0.68766 126 ->128 0.12409
5	3.2948 eV 376.31 nm	0.2003	120 ->127 -0.11311 122 ->127 0.66767 126 ->127 0.15436
6	3.8230 eV 324.31 nm	0.0374	121 ->127 0.67256 126 ->128 0.19240
7	3.9471 eV 314.12 nm	0.2207	120 ->127 0.67634 122 ->127 0.14309
8	4.0658 eV 304.94 nm	0.0999	124 ->128 0.17551 125 ->129 -0.11688 126 ->129 0.65431
9	4.1374 eV 299.67 nm	0.1029	121 ->127 -0.15308 125 ->128 0.15213 125 ->130 0.13391 126 ->128 0.54563 126 ->130 -0.31262
10	4.3419 eV 285.55 nm	0.0241	119 ->127 -0.16854 125 ->128 -0.38748 126 ->128 0.32090 126 ->130 0.42131
11	4.4121 eV 281.01 nm	0.0438	118 ->127 0.64041 119 ->128 0.11097 126 ->131 -0.21810
12	4.4154 eV 280.80 nm	0.0065	118 ->128 0.11280 119 ->127 0.65939 125 ->128 -0.12183
13	4.4270 eV 280.06 nm	0.1415	118 ->127 0.23599 124 ->128 -0.22242 125 ->129 0.14823 126 ->129 0.13103

Excited State	Energy	Oscillator Strength (f)	Orbitals and coefficients (126=HOMO, 127=LUMO)
14	4.4898 eV 276.15 nm	0.0074	126 ->131 0.57015
			123 ->129 -0.14255
			125 ->128 0.51166
15	4.5727 eV 271.14 nm	0.0682	126 ->130 0.42599
			124 ->128 -0.37618
			125 ->129 0.45781
			126 ->129 0.16650
16	4.6165 eV 268.57 nm	0.1604	126 ->131 -0.29933
			123 ->130 0.11970
			124 ->128 0.46833
			125 ->129 0.47906
17	4.6840 eV 264.70 nm	0.0121	123 ->129 0.40105
			124 ->129 0.53226
			125 ->128 0.12570
18	4.7297 eV 262.14 nm	0.0382	123 ->128 0.61430
			123 ->130 -0.12628
			124 ->130 -0.10480
			125 ->131 0.22675
			126 ->132 -0.12517
19	4.7578 eV 260.59 nm	0.0245	123 ->128 0.12605
			126 ->132 0.67608
20	4.7624 eV 260.34 nm	0.0037	123 ->129 -0.40281
			124 ->129 0.28813
			124 ->131 -0.13911
			125 ->130 0.44934
			126 ->130 0.10665

References:

- (1) Becke, A. D. *J. Chem. Phys.* **1997**, *98*, 5648-5652.
- (2) Tomasi, J.; Mennucci, B.; Cammi, R. *Chem. Rev.* **2005**, *105*, 2999-3093.
- (3) Frisch, M. J., G. W. T., H. B. Schlegel, G. E. Scuseria, M. A. Robb, J. R. Cheeseman, G. Scalmani, V. Barone, B. Mennucci, G. A. Petersson, H. Nakatsuji, M. Caricato, X. Li, H. P. Hratchian, A. F. Izmaylov, J. Bloino, G. Zheng, J. L. Sonnenberg, M. Hada, M. Ehara, K. Toyota, R. Fukuda, J. Hasegawa, M. Ishida, T. Nakajima, Y. Honda, O. Kitao, H. Nakai, T. Vreven, J. A. Montgomery, Jr., J. E. Peralta, F. Ogliaro, M. Bearpark, J. J. Heyd, E. Brothers, K. N. Kudin, V. N. Staroverov, R. Kobayashi, J. Normand, K. Raghavachari, A. Rendell, J. C. Burant, S. S. Iyengar, J. Tomasi, M. Cossi, N. Rega, J. M. Millam, M. Klene, J. E. Knox, J. B. Cross, V. Bakken, C. Adamo, J. Jaramillo, R. Gomperts, R. E. Stratmann, O. Yazyev, A. J. Austin, R. Cammi, C. Pomelli, J. W. Ochterski, R. L. Martin, K. Morokuma, V. G. Zakrzewski, G. A. Voth, P. Salvador, J. J. Dannenberg, S. Dapprich, A. D. Daniels, Ö. Farkas, J. B. Foresman, J. V. Ortiz, J. Cioslowski, and D. J. Fox; Gaussian, Inc.: Wallingford CT, 2009.
- (4) Stratmann, R. E.; Scuseria, G. E.; Frisch, M. J. *J. Chem. Phys.* **1998**, *109*, 8218-8224.
- (5) Dennington, R.; Keith, T.; Millam, J. M.; Semichem Inc.: Shawnee Mission KS, 2009.
- (6) Hehre, W. J.; Wavefunction Inc.: Irvine, CA, 2009.